PROCEEDINGS OF SCIENCE

Measurements of Vector Meson Global Spin Alignment in Heavy-Ion Collisions at RHIC

Gavin M. Wilks for the STAR Collaboration

University of Illinois at Chicago,
1200 W Harrison, Chicago, IL 60607, United States of America

E-mail: gwilks3@uic.edu

STAR collaboration observed a global spin alignment of ϕ-mesons in Au+Au collisions using the data from the first phase of the RHIC Beam Energy Scan program (BES- I) [1]. This cannot be explained by conventional mechanisms but may be attributable to the influence of vector meson force fields. In these proceedings, we present new differential measurements of ϕ-meson global spin alignment with respect to transverse momentum (p_T), centrality, and rapidity (y) using higher-statistics Au+Au data at $\sqrt{s_{\mathrm{NN}}}$ = 14.6 and 19.6 GeV from the BES-II program. These differential measurements can help understand the roles of the ϕ-meson force field in nucleon and nuclear structure, in addition to the evolution of nuclear matter.

25th International Spin Physics Symposium (SPIN 2023)
24-29 September 2023
Durham, NC, USA

1. Introduction

Particle polarization has gained much interest in recent years as a tool for probing various properties of Quark Gluon Plasma (QGP). At the non-central (not directly head on) heavy-ion collisions, a large orbital angular momentum is generated, leading to vorticity of the QGP along the orbital angular momentum direction. This can lead to polarization of particle spin through spin-orbit couplings [2], termed global polarization. Since the polarization of the $\Lambda(\bar{\Lambda})$ hyperon is carried only by the strange quark $s(\bar{s})$ according to the flavour-spin wave function, we can probe the $s(\bar{s})$ global polarization with $\Lambda(\bar{\Lambda})$ hyperons [3]. Global polarization can be measured for $\Lambda(\bar{\Lambda})$ hyperons since they decay through the weak force with parity violation, where the decay products are preferentially emitted in the spin direction. Recently, the STAR Collaboration has measured a significant signal of $\Lambda(\bar{\Lambda})$ hyperon global polarization [4].

In the quark coalescence model, the production of ϕ-meson ($s\bar{s}$) is affected by the global polarization of the $s(\bar{s})$ [5]. An analog to the global polarization for vector mesons is the global spin alignment, which can indirectly measure the polarization of vector mesons since they primarily decay through the strong interaction, where parity is conserved. Global spin alignment is measured by the ρ_{00} diagonal element of the spin density matrix, which is associated with the tensor polarization, T_{ij}. For a ϕ-meson undergoing the strong decay of $\phi \to K^+K^-$, the K^+ or K^- daughter's polar angle (θ^*) distribution within the ϕ-meson rest frame is given by:

$$\frac{dN}{d(\cos\theta^*)} \propto (1-\rho_{00}) + (3\rho_{00}-1)\cos^2\theta^*. \tag{1}$$

If $\rho_{00} \neq 1/3$, then the spin states of the ϕ-meson are not equally probable, resulting in an anisotropic polar angle distribution of the daughter kaon. When $\rho_{00} > 1/3$, the occupation of the spin 0 state is more probable, corresponding to an alignment of the ϕ-meson's average polarization along the spin-quantization axis. Conversely, when $\rho_{00} < 1/3$, the occupation of the spin -1 or 1 states are more probable, corresponding an alignment of the average polarization along the normal of the spin-quantization axis [6, 7].

The s and $\bar{s}$ quarks can be polarizated from the electromagnetic fields generated by the colliding nuclei and the vortical flow of the QGP, both contributing to the global spin alignment of ϕ-mesons [2, 5, 8]. Other conventional contributions to ρ_{00} include: helicity polarization [9], fragmentation of polarized quark [2], locally fluctuating axial charge currents [10], and local vorticity loops [11]. Estimates of these contributions are at most on the order of a few times 10^{-4} above 1/3. Recent STAR measurements [1] report a significant signal of ϕ-meson $\rho_{00} > 1/3$ in mid-central Au+Au collisions from the first phase of the Beam Energy Scan at RHIC (BES-I) at energies below $\sqrt{s_{\mathrm{NN}}}$ = 62.4 GeV on the order of 2×10^{-2} above 1/3. In [5], it was proposed that fluctuations of the theoretical ϕ-meson strong force field can accommodate the large ρ_{00} signal from STAR. The connection between a possible ϕ-meson field and the ϕ-meson global spin alignment would allows us to probe features of field, which were previously inaccessible. In these proceedings, we report ϕ-meson ρ_{00} measurements from Au+Au collisions from the second phase of the Beam Energy Scan at RHIC (BES-II) at $\sqrt{s_{\mathrm{NN}}}$ = 14.6 and 19.6 GeV. The increased statistics in BES-II allow more precision and differential measurements which were not possible from BES-I.

2. Analysis Details

In this analysis, we study Au+Au collisions at $\sqrt{s_{\mathrm{NN}}}$ = 14.6 and 19.6 GeV from the BES-II program measured by the STAR detector. The BES-II STAR data includes 324 million and 478 million events for 14.6 and 19.6 GeV, respectively. This is significantly larger than the BES-I STAR data with 18 million and 36 million events for 14.6 and 19.6 GeV, respectively. In addition to increased statistics, many upgrades were made to the STAR detector in preparation of BES-II, including an Event Plane Detector (EPD) [12] and an inner Time Projection Chamber (iTPC) upgrade [13]. These detector upgrades and the increased statistics improve the precision of our BES-II measurements compared to previous BES-I measurements.

2.1 Experimental determination of the spin-quantization axis

As discussed, global spin alignment corresponds to a vector meson's average polarization along spin-quantization axis. In this analysis, we will define the spin-quantization axis as the orbital angular momentum direction in each event, as we need an axis where the projection of angular momentum has well-defined quantum numbers. The orbital angular momentum direction corresponds to the normal of the reaction plane spanned by the impact parameter vector and the initial direction of the colliding nuclei. In data, the true reaction plane angle can not be known, but it can be estimated by the first- and second-order harmonic event planes calculated through methods discussed in [14]. We use the first- and second-order harmonic event planes as individual estimations of the reaction plane and calculate the θ^* angle of the K^+ decay daughter with respect to the normal of each plane.

2.2 ϕ-meson yield extraction

This analysis used data collected by the STAR detector, which provides full azimuthal coverage in the pseudo-rapidity region $|\eta| < 1.5$. In this analysis we restrict our detector coverage to $|\eta| < 1$ to remain consistent with previous STAR results from BES-I and we will extend measurements to $|\eta| < 1.5$ in the future. We require that our events in this analysis have a primary vertex located within 70 cm along the beam axis and within 2 cm in the transverse plane from the center of STAR. The Time Projection Chamber (TPC) with the iTPC upgrade for BES-II were used for centrality determination, particle tracking and identification, and second-order event plane reconstruction. The Time-of-Flight (TOF) detector was used for invariant mass constraints for improved particle identification (PID). Lastly, the EPD was used for first-order event plane reconstruction. Using the TPC+iTPC and TOF sub-detector systems, we identify kaon candidates and combine K^+ and K^- in a given event to generate our signal+background invariant mass distribution (same-event). The mixed-event method is used to generate the combinatorial background invariant mass distribution, where K^+ and K^- are combined from different events with similar centralities, primary vertices, and event planes. The mixed-event background is normalized to the right tail of the same-event distribution and then subtracted, leaving us with a signal and residual background. To extract the raw ϕ-meson yield we fit this final invariant mass distribution using the sum of a Breit-Wigner function for the signal and a third-order polynomial for the residual background. In this analysis, 7 bins in $|\cos\theta^*|$ from 0 to 1 are used for ρ_{00} extraction in each p_T, centrality, and $|y|$ bin combination.

The fit to the invariant mass distribution integrated over $|\cos\theta^*|$ sets the center (m_ϕ) and width (Γ) values of fits for individual $|\cos\theta^*|$ bins.

2.3 Acceptance and efficiency correction of yields

Two sources of efficiency loss are accounted for in this analysis. The first being the TPC tracking efficiency of K^+ and K^- daughter particles. The standard STAR embedding technique is used to simulate kaons within our data and uses a simulated STAR detector for realistic detector effects. The second efficiency loss is from the matching of TPC tracks to the TOF. In this anlysis, each kaon track candidate is required to satisfy TPC tracking constraints and have matching hits within the TOF simultaneously. Using data, stringent cuts are applied on the PID information from the TPC to select a nearly pure kaon sample and then we apply the matching TOF hit requirement on these selected tracks. The ratio after to before the matching TOF hit requirement determines our TOF matching efficiency.

Since the $|\cos\theta^*|$ dependence of efficiency and acceptance ($A \times \epsilon$) is required to correct the ϕ-meson yields as a function of $|\cos\theta^*|$, we use a Monte-Carlo (MC) model with Pythia6 decays of ϕ-meson. The first step is to smear the event plane using the known resolutions in each centrality bin from our data, as this will affect the $|\cos\theta^*|$ values which need to match the data. Using published, preliminary, or interpolated data of p_T dependent elliptic flow and p_T spectra, we generate the input kinematics for MC ϕ-mesons. The rapidity input is modeled as a uniform distribution for $-1 < y < 1$ in this simulation. The ϕ-mesons decay into kaon pairs via Pythia6 and the TPC tracking and TOF matching efficiencies are applied. The detector geometry acceptance cut of $|\eta| < 1$ is also applied on each of the kaon daughters. The ratio of reconstructed to MC ϕ-mesons, which is equivalent to $A \times \epsilon$, can then be calculated as a function of $|\cos\theta^*|$. The raw yields are finally corrected by dividing by $A \times \epsilon$.

2.4 Extraction of ρ_{00} and the event plane resolution correction

Following the $A \times \epsilon$ correction, the observed global spin alignment ρ_{00}^{obs} can be measured by fitting the $|\cos\theta^*|$ dependent yields (N^{corr}) with the following function:

$$\frac{dN^{corr}}{d(|\cos\theta^*|)} = Norm. \times \left[(1-\rho_{00}^{obs}) + (3\rho_{00}^{obs}-1)|\cos\theta^*|^2\right], \tag{2}$$

where we rewrite Equation 1 in terms of $|\cos\theta^*|$, given that it is an even function.

The ρ_{00}^{obs} is affected by the ability of the detectors to reconstruct the event plane; also known as the event plane resolution, R. Following the methods described in [15], we correct the ρ_{00}^{obs} with the general formula,

$$\rho_{00} = \frac{1}{3} + \frac{4}{1+3R}\left(\rho_{00}^{obs} - \frac{1}{3}\right). \tag{3}$$

Note that R is different for first- and second-order event plane and a modified value R_{21} is used for the second-order results to ensure they are compatible with the first-order results. See [15] for details.

3. Results and discussion

3.1 $\sqrt{s_{NN}}$ dependence of ρ_{00}

Figure 1 shows the collision energy dependence of ϕ-meson ρ_{00} for mid-central (20-60% centrality) BES-II Au+Au collisions at $\sqrt{s_{\rm NN}}$ = 14.6 and 19.6 GeV. The results for $\sqrt{s_{\rm NN}}$ = 19.6 GeV from BES-I and BES-II are consistent for the first- and second-order event plane methods. The improved statistics from the BES-II program have increased the precision, and therefore, the significance of our measurement of $\rho_{00} > 1/3$ at this energy. The first results for $\sqrt{s_{\rm NN}}$ = 14.6 GeV are reported and are consistent with $\rho_{00} > 1/3$. The solid line is a fit only to BES-I data and is derived from the ϕ-meson strong force field model discussed in [5, 16].

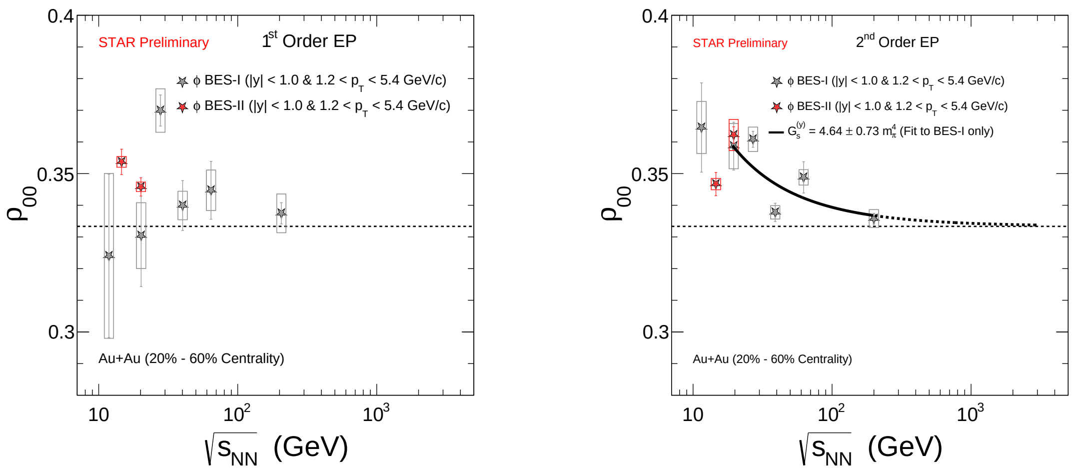

Figure 1: $\sqrt{s_{\rm NN}}$ dependent ϕ-meson ρ_{00} with $|y| < 1$ and $1.2 < p_T < 5.4$ GeV/c for 20-60% centrality Au+Au collisions. Results are shown for measurements relative to the first-order (left) and second-order (right) event planes, and for BES-I (grey stars) and BES-II (red stars) data. The solid black line represents the fit to the BES-I data from [1] an the dashed black line is an extrapolation of the fit. The parameter G_s^y is the free parameter of the fit and further details can be found in [1]. The vertical lines are statistical uncertainties and boxes represent systematic uncertainties.

3.2 p_T dependence of ρ_{00}

The p_T dependent ϕ-meson global spin alignment from the first- and second- order event plane methods are presented in Figure 2 for BES-II mid-central Au+Au collisions at $\sqrt{s_{\rm NN}}$ = 14.6 GeV. The results from the first- and second-order event planes are consistent and no significant dependence on p_T is observed.

3.3 Centrality dependence of ρ_{00}

In Figure 3, the centrality dependence of ϕ-meson ρ_{00} is shown for the first- and second-order event plane methods in BES-II Au+Au collisions at $\sqrt{s_{\rm NN}}$ = 14.6 and 19.6 GeV. The results for different event planes are consistent and there is no significant dependence of ρ_{00} on centrality. This is in contrast to results that are seen for $\Lambda(\bar{\Lambda})$ polarization where there is strong dependence

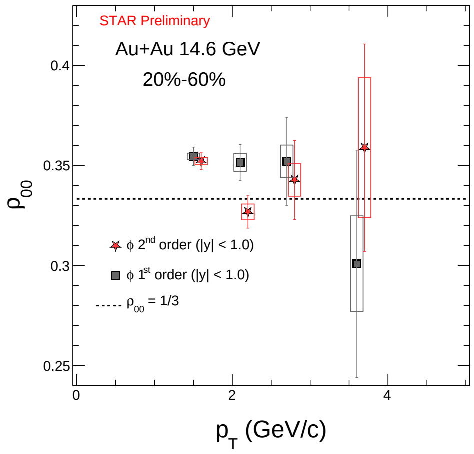

Figure 2: p_T dependent ϕ-meson ρ_{00} with $|y| < 1$ for 20-60% centrality BES-II Au+Au collisions at $\sqrt{s_{\mathrm{NN}}}$ = 14.6 GeV. Results using first-order (grey squares) and second-order (red stars) event planes are shown. The vertical lines are statistical uncertainties and boxes represent systematic uncertainties.

on centrality [17, 18]. For $\Lambda(\bar{\Lambda})$, an increase in global polarization is expected at higher values of centrality where larger orbital angular momentum is expected. This is consistent with the theoretical predictions of contributions to ϕ-meson global spin alignment, where only a small contribution is predicted from the magnetic components of the electromagnetic and vorticity fields, considered as the only physical mechanisms which contribute to both $\Lambda(\bar{\Lambda})$ polarization and ϕ-meson global spin alignment [5].

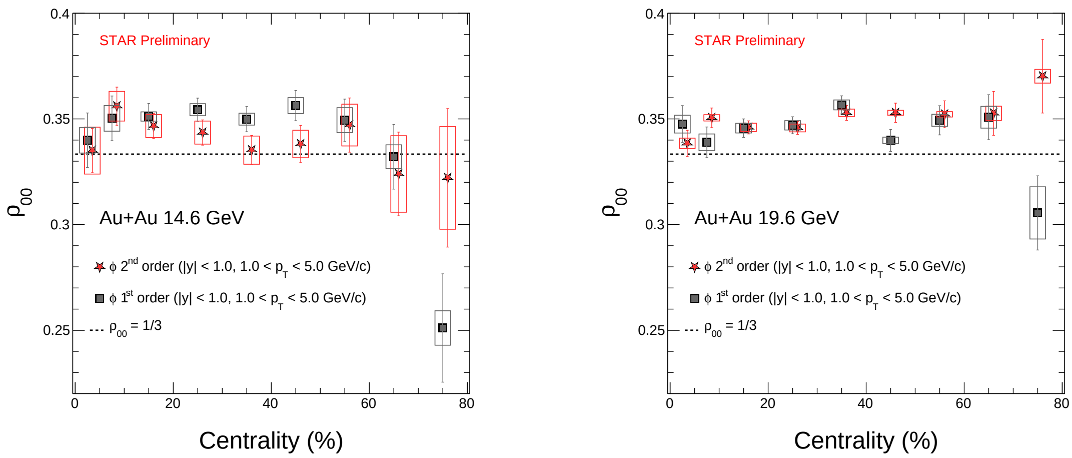

Figure 3: Centrality dependent ϕ-meson ρ_{00} with $|y| < 1$ and $1 < p_T < 5$ GeV/c for BES-II Au+Au collisions at $\sqrt{s_{\mathrm{NN}}}$ = 14.6 GeV (left) and 19.6 GeV (right). Results using first-order (grey squares) and second-order (red stars) event planes are shown. The vertical lines are statistical uncertainties and boxes represent systematic uncertainties.

3.4 $|y|$ dependence of ρ_{00}

The first measurements of rapidity dependence of ϕ-meson ρ_{00} are presented in Figure 4. The results are shown for ϕ-mesons in 0-80% centrality BES-II Au+Au collisions at $\sqrt{s_{\mathrm{NN}}}$ = 14.6 and 19.6 GeV for the first- and second-order event plane methods. For both energies and event planes, we observe $\rho_{00} = 1/3$ at mid-rapidity ($|y| = 0$) and an increasing trend as $|y|$ approaches 1. Using BES-I data for in-plane (with respect to the reaction plane) and out-of-plane (with respect to normal of the reaction plane) ρ_{00}, predictions of the $|y|$ dependence were made in [19]. The prediction for $\sqrt{s_{\mathrm{NN}}}$ = 19.6 GeV can be seen in Figure 4 and is consistent with our data for $|y| > 0.5$. These predictions follow directly from the ϕ-meson strong force field model discussed in [5, 16]. The current understanding in this model is that anisotropies in the ϕ-meson field fluctuations can cause ρ_{00} to deviate from 1/3. Consider $|y|$ = 1, where a large portion of the ϕ-meson momentum would lie along the beam direction (z axis) within the lab frame. When boosting to the ϕ-meson rest frame, we would see a suppression in the field fluctuations along the beam direction, leading to larger anisotropy between the fluctuations along the orbital angular momentum direction (-y axis) and the beam direction. The increased anisotropy with increasing $|y|$ will lead to a larger global alignment along the orbital angular momentum direction and thus, $\rho_{00} > 1/3$ [19].

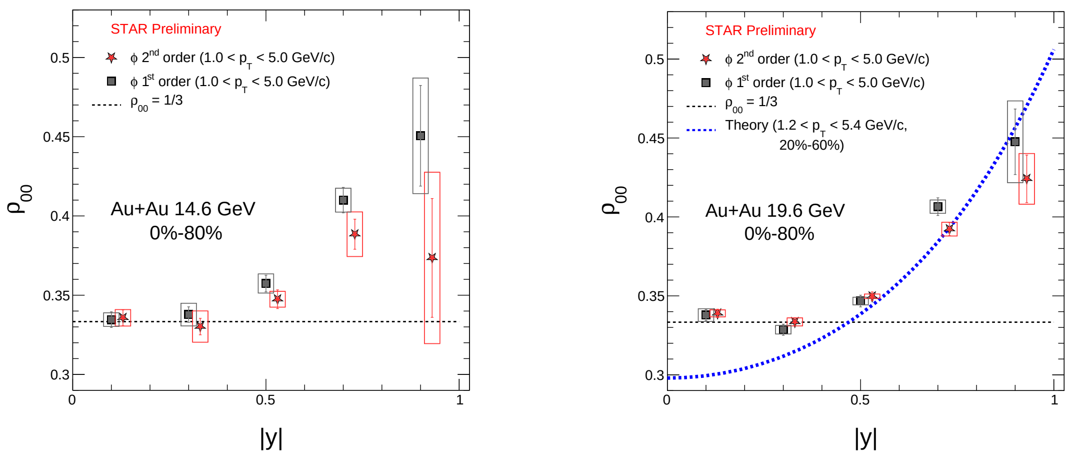

Figure 4: Rapidity dependent ϕ-meson ρ_{00} with $1 < p_T < 5$ GeV/c for 0-80% centrality BES-II Au+Au collisions at $\sqrt{s_{\mathrm{NN}}}$ = 14.6 GeV (left) and 19.6 GeV (right). Results using first-order (grey squares) and second-order (red stars) event planes are shown. The blue dashed lines represents the prediction from the ϕ-meson strong force field model in [19]. The vertical lines are statistical uncertainties and boxes represent systematic uncertainties.

4. Conclusion

We have presented measurements of ϕ-meson global spin alignment with respect to the first- and second-order event planes for BES-II Au+Au collisions at $\sqrt{s_{\mathrm{NN}}}$ = 14.6 and 19.6 GeV. Integrated values of ϕ-meson ρ_{00} over p_T at $\sqrt{s_{\mathrm{NN}}}$ = 19.6 GeV are consistent for BES-I and BES-II data. There is no significant dependence of ϕ-meson ρ_{00} on p_T or the collision centrality. The first measurements of ϕ-meson ρ_{00} rapidity dependence are reported with no spin alignment at mid-rapidity and increasing ρ_{00} with rapidity ($|y| > 0.5$) for both energies. The predictions at $\sqrt{s_{\mathrm{NN}}}$ = 19.6 GeV from a theoretical ϕ-meson strong force field model are compared to our data and shows consistency for $|y| > 0.5$ [19]. All studies show consistency between the first- and second-order event plane results. Further studies will include the remaining collision energies from the BES-II program and an expanded $|\eta|$ acceptance window. This work explores the potential link between the ϕ-meson field and global spin alignment, and aims to guide theoretical developments towards understanding vector meson fields.

Acknowledgements

The author is supported in part by the United States Department of Energy (DOE) Office of Science.

References

[1] STAR Collaboration, Nature **614** 244-248 (2023).

[2] Liang et al., Phys. Lett. B **629**, 20–26 (2005).

[3] Close, *An Introduction to Quarks and Partons*, Academic Press (1979).

[4] STAR Collaboration, Nature **548**, 62–65 (2017).

[5] Sheng et al., Phys. Rev. D **101**, 096005 (2020).

[6] Schilling et al., Nucl. Phys. B **18**, 332 (1970).

[7] Chen et al., Science Bulletin **68** 874–877 (2023).

[8] Yang et al., Phys. Rev. C **97**, 034917 (2018).

[9] Gao et al., Phys. Rev. D **104**, 076016 (2021).

[10] Müller et al., Phys. Rev. D **105**, L011901 (2022).

[11] Xia et al., Phys. Lett. B **817**, 136325 (2021).

[12] STAR Collaboration, STAR Note 619, https://drupal.star.bnl.gov/STAR/starnotes/public/sn0619

[13] STAR Collaboration, STAR Note 666, https://drupal.star.bnl.gov/STAR/starnotes/public/sn0666

[14] Poskanzer et al., Phys. Rev. C **58**, 1671–1678 (1998).

[15] Tang et al., Phys. Rev. C **98**, 044907 (2018). [Erratum: Phys. Rev. C **107**, 039901 (2023).]

[16] Sheng et al., Phys. Rev. D **102**, 056013 (2020).

[17] STAR Collaboration, Phys. Rev. C **98**, 014910 (2018).

[18] STAR Collaboration, arXiv:2305.08705 (2023).

[19] Sheng et al., Phys. Rev. C **108**, 054902 (2023).